JACS Au
AN OPEN ACCESS JOURNAL OF THE AMERICAN CHEMICAL SOCIETY

pubs.acs.org/jacsau
Article

EF-Hand Battle Royale: Hetero-ion Complexation in Lanmodulin

Jeremy Seidel, Patrick Diep, Ziye Dong, Joseph A. Cotruvo, Jr., and Dan M. Park*

Cite This: JACS Au 2024, 4, 4273−4284
Read Online

ACCESS | Metrics & More | Article Recommendations | Supporting Information

ABSTRACT: The lanmodulin (LanM) protein has emerged as an effective means for rare earth element (REE) extraction and separation from complex feedstocks without the use of organic solvents. Whereas the binding of LanM to individual REEs has been well characterized, little is known about the thermodynamics of mixed metal binding complexes (i.e., heterogeneous ion complexes), which limits the ability to accurately predict separation performance for a given metal ion mixture. In this paper, we employ the law of mass action to establish a theory of perfect cooperativity for LanM-REE complexation at the two highest-affinity binding sites. The theory is then used to derive an equation that explains the nonintuitive REE binding behavior of LanM, where separation factors for binary pairs of ions vary widely based on the ratio of ions in the aqueous phase, a phenomenon that is distinct from single-ion-binding chemical chelators. We then experimentally validate this theory and perform the first quantitative characterization of LanM complexation with heterogeneous ion pairs using resin-immobilized LanM. Importantly, the resulting homogeneous and heterogeneous constants enable accurate prediction of the equilibrium state of LanM in the presence of mixtures of up to 10 REEs, confirming that the perfect cooperativity model is an accurate mechanistic description of REE complexation by LanM. We further employ the model to simulate separation performance over a range of homogeneous and heterogeneous binding constants, revealing important insights into how mixed binding differentially impacts REE separations based on the relative positioning of the ion pairs within the lanthanide series. In addition to informing REE separation process optimization, these results provide mathematical and experimental insight into competition dynamics in other ubiquitous and medically relevant, cooperative binding proteins, such as calmodulin.

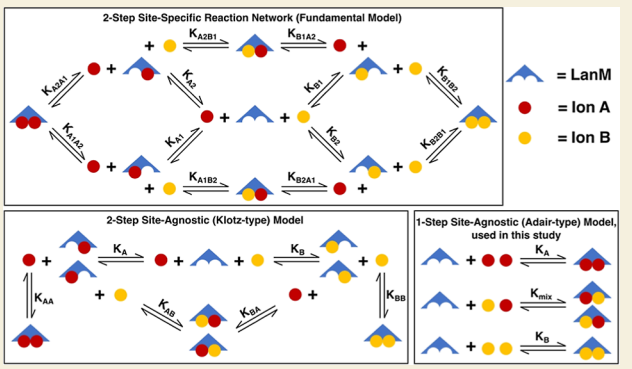

KEYWORDS: *lanmodulin, REE separation, rare earths, mixed binding, lanmodulin reaction network, mixed metal binding, poly-ion model, separation factor*

INTRODUCTION

The lanthanides along with yttrium and scandium, collectively known as rare earth elements (REEs), possess unique physical properties that have made them critical to consumer electronic devices, military technology, and clean energy technologies. As the global economy becomes more reliant on renewable energy sources, REE demand is expected to grow at a compound annual growth rate of 8.3% between 2023 and 2027.[1] Despite their critical importance to modern life, REE recovery and extraction is still dependent on solvent-based mixer-settler processes established in the 1940s−1960s.[2] Mixer-settler processes are capital intensive and pose significant environmental and health hazards due to their reliance on organic solvents.[3] To mitigate these risks and reduce the cost of REE production, it is critical to develop new technologies for REE extraction and purification.

In recent years, biomolecules have been increasingly recognized for their potential as selective ligands for the recovery and separation of REEs. Lanthanide binding tags (LBTs)[4] were originally developed for the purpose of tagging proteins with terbium luminescence for biomedical studies, but their precise engineering for lanthanide selectivity garnered interest in their utility for REE extractions.[5,6] However, LBTs were limited by lack of tolerance to industrially relevant acidic conditions, their low intra-REE selectivity from Sm through Yb, and the difficulty of producing short peptides industrially.[7,8] The recent discovery of lanmodulin (LanM) from *Methylobacterium (Methylorubrum) extorquens* and its orthologs in other organisms has provided proteins with high selectivity for REEs as well as useful intra-REE selectivity.[9−12] Recent work with LanM-functionalized agarose has demonstrated successful separation of mixtures of Nd(III) and Dy(III) present in rare earth magnets as well as Sc(III) and Y(III) from more complex REE mixtures characteristic of ore leachates.[10−12] However, immobilized LanM-based separations have

Received: July 15, 2024
Revised: August 15, 2024
Accepted: August 19, 2024
Published: September 5, 2024

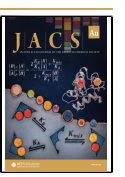

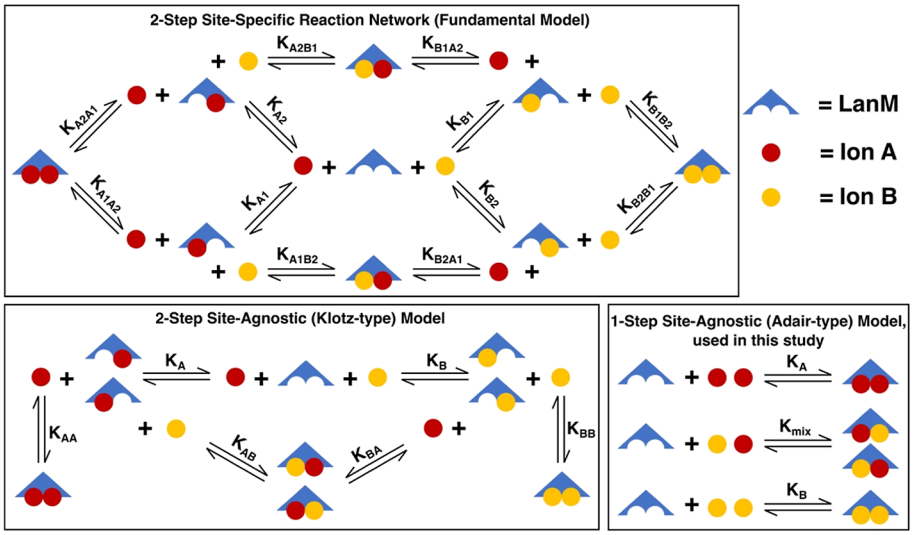

Figure 1. Reaction networks of varying complexity describing lanthanide ions competing for binding sites on LanM. The full reaction network was previously proposed by Malmendal et al. to explain calcium−magnesium competition in calmodulin.[16] This work employs the Adair-type model to characterize mixed binding of over 60 hetero-ion complexes with LanM.

so far been designed and optimized in a fully empirical manner, which limits the potential for rigorous scale-up and process optimization. A precise quantitative understanding of LanM, especially in its immobilized form, is critical for developing a predictive model for REE separations.

Prior work measuring LanM's affinity for REEs has focused on the free protein, using circular dichroism to measure LanM folding in the presence of chelator-controlled, single REE ion solutions. LanM was shown to have a 3:1 binding stoichiometry at neutral pH. EF-hand 1 is substantially weakened at pH 5 and lower, effectively reducing the complexation stoichiometry to 2:1, with binding occurring to the highest-affinity EF hands (EF2 and EF3).[9,13] These studies revealed that LanM's complexation of the first two binding equivalents is highly cooperative and favors light REEs, especially Nd and Sm, compared to heavy REEs.[9,14] Equilibration of immobilized LanM with equimolar mixtures of REEs confirmed that the preference for these lanthanides is conserved after immobilization.[10−12] This preference has proven particularly useful in column-based separations because it allows LanM to synergize with the separation capabilities of organic chelators, such as citrate, EDTA, and DTPA, which typically favor heavy REEs.[11,12,15] Immobilized LanM has been shown to have a 2:1 binding stoichiometry, with binding thought to occur within EF hands 2 and 3,[11] on the basis of solution studies.[14] Characterization of immobilized LanM has been limited to binding of equimolar or feedstock-relevant mixtures of many REEs.[12] While this work has largely agreed with the trends revealed by work on free LanM, it is difficult to disentangle the interplay of mixed solutions of REEs cooperatively binding to LanM.

The presence of multiple REE binding sites raises the distinct possibility that LanM forms mixed REE complexes (hereafter referred to as heterogeneous complexes), where LanM's affinity for a particular ion is impacted by which other ion(s) are bound to the same protein. Indeed, prior work characterizing the ubiquitous EF-hand protein calmodulin has shown that Ca binding is affected by Mg co-binding.[16] A more recent spectrophotometry study of LanM-REE complexes suggested the formation of mixed complexes but did not further interrogate this phenomenon.[13] We posit that rigorous characterization of heterogeneous binding is critical for developing an accurate process model for REE separations and for better understanding the physiological role of LanM inside the cell, where it is more likely to encounter heterogeneous ion pairs rather than homogeneous ion pairs given the geological co-occurrence of REEs. More broadly, characterizing mixed binding in LanM presents a unique opportunity to develop a mathematical and experimental framework that could be employed to better understand factors that influence heterogeneous ligand complexation in other cooperative binding proteins, such as calmodulin.

In this work, we develop a mathematical model for cooperative binding of heterogeneous REE pairs to LanM. By quantitatively characterizing the REE binding of LanM and its variants in mixed REE solutions, we determined the mixed binding constants for all pairwise combinations of 10 REEs and show that these constants enable the accurate prediction of adsorption activity in complex mixtures of REEs. This work reveals important insights into the origins of REE selectivity in LanM and provides a critical step toward process modeling and scale-up for a LanM-based REE separation process.

THEORY

There are many empirical and theoretical models for cooperative binding proteins in the literature, most notably by Hill (1910), Adair (1925), and Klotz (1946).[17−19] The Hill equation is of limited utility in theoretical models because the binding constant and Hill coefficient cannot be directly linked to specific complexation events and instead represent the aggregate effect of many binding events. By contrast, Adair's model is derived directly from the law of mass action, with each constant representing the equilibrium constant for the formation of each complex.[18] The Klotz model is also derived from the law of mass action. However, unlike Adair's model, Klotz described the reaction in stepwise binding events starting with the formation of a single-ion complex and progressing to higher-order complexes, one ion at a time.[19] The model presented here starts as a simplified version of the second-order Adair model of cooperativity in which the stability of the

https://doi.org/10.1021/jacsau.4c00628
JACS Au 2024, 4, 4273−4284

single−ligand complex is assumed to be sufficiently less stable than the two-ion complex that it can be neglected. An algebraic derivation is then employed to expand the Adair model to describe two ions competing to form homogeneous and heterogeneous ion complexes with LanM. Similar to the Adair model, this LanM model cannot account for single-ion or two-ion complex stability. Instead, equilibrium constants reported are the product of the single-ion and two-ion complex equilibrium formation constants. Due to technical limitations inherent in using mass balances to determine ion partitioning, these data do not allow us to deconvolute the single-ion and two-ion complexation steps like the Klotz model.

We begin our theoretical exploration of LanM's lanthanide-separation ability by defining a rigorous reaction network for two competing ions, A and B, for EF-hand domains 2 and 3 (Figure 1). This reaction network includes individual equilibrium constants for each EF-hand to sequentially form single-ion and two-ion complexes in all possible configurations. While theoretically sound, this reaction network presents a near-insurmountable practical challenge: distinguishing between binding to either EF-hand 2 or 3 without low-throughput experiments (e.g., X-ray crystallography, NMR). The partial reaction network is a simplification that ignores site-specificity by lumping both orientations of each complex together while retaining the sequential path from single-ion complex to two-ion complex. Here, LanM presents a particular challenge for determining the single-ion complexation dynamics: the two-ion complex is sufficiently stable that the single-ion complex is too dilute to be accurately measured-a limitation that must be accommodated in the modeling approach. Finally, we arrive at the most simplified version of the reaction network in which only the two-ion complexes are present. While this reaction network yields constants that we may determine experimentally, it is important to note that these equilibrium constants are the product of several intermediate reaction equilibrium constants. As such, these equilibrium constants are not a direct measure of complex stability; however, they are sufficient to accurately predict equilibrium protein binding for a large variety of REE ion mixtures consisting of two or more ions (vide infra).

In this work, we endeavor to validate the simple reaction network model. This model assumes that immobilized LanM is perfectly cooperative with a 2:1 stoichiometry, leading to a system of four equations when two different REEs are competing for binding sites. The reactions for ions A and B binding to LanM, generalized as protein P, to generate protein-ion complexes P^*A_2, P^*B_2, P*AB, and P*BA are presented as follows

$$P + 2A \rightleftharpoons P^*A_2$$

$$P + 2B \rightleftharpoons P^*B_2$$

$$P + A + B \rightleftharpoons P^*AB$$

$$P + A + B \rightleftharpoons P^*BA$$

While two configurations exist for the heterogeneous ion complex, we are unable to differentiate them with our experimental methods. For this reason, the formation of P*AB and P*BA are combined into one reaction where P*AB will be used to refer to both for simplicity. By applying the law of mass action, we then convert this system of chemical reactions into a system of algebraic equations where the K variables correspond to the equilibrium coefficients for the formation of each respective proteinion complex.

$$K_A = \frac{[P^*A_2]}{[P][A]^2} \tag{1}$$

$$K_B = \frac{[P^*B_2]}{[P][B]^2} \tag{2}$$

$$K_{mix} = \frac{[P^*AB]}{[P][A][B]} \tag{3}$$

Equations 1−3, although theoretically valid, present a vexing experimental challenge: it is difficult to accurately determine the binding coefficient of strong complexes like those formed between LanM and REEs. In an experimental sense, it is difficult to precisely determine the amount of free protein in equilibrium with REE ions in excess. Fortunately, it is possible to exclude the free protein concentration from calculations by using ratios of equilibrium constants rather than the constants themselves, resulting in eqs 4 and 5. A mass balance for the protein is necessary to complete the system of equations. If REE ions were not in excess of the protein, we would face a similar challenge in determining the free ion concentration, so we performed all experiments with 50-fold excess REEs. As a result, we may assume that the free protein concentration is zero for the mass balance (eq 6). This results in a system of three algebraic equations

$$R_B = \frac{K_B}{K_A} = \frac{[P^*B_2][A]^2}{[P^*A_2][B]^2} \tag{4}$$

$$R_{mix} = \frac{K_{AB}}{K_A} = \frac{[P^*AB][A]}{[P^*A_2][B]} \tag{5}$$

$$[P]_{total} = [P^*A_2] + [P^*B_2] + [P^*AB] \tag{6}$$

Once again, we are presented with unmeasurable quantities: the concentrations of the three LanM complexes. However, we can measure the total amount of each ion bound to the protein by direct ion quantification after desorbing the bound ions. This necessitates the inclusion of mass balances for each protein-bound ion alongside the definition of separation factor (SF)

$$SF_{B/A} \equiv \frac{[A]}{[B]} \cdot \frac{[B]_{protein}}{[A]_{protein}} \tag{7}$$

$$[A]_{protein} = 2\cdot[P^*A_2] + [P^*AB] \tag{8}$$

$$[B]_{protein} = 2\cdot[P^*B_2] + [P^*AB] \tag{9}$$

By combining eqs 4−9, we obtain a system of six equations with six unknown variables: $SF_{B/A}$, R_A, R_{mix}, $[P^*A_2]$, $[P^*B_2]$ and [P*AB]. These equations can be simplified to eq 10 through algebraic operations as shown in the Supporting Information.

$$SF_{B/A} = \frac{2R_B\left(\frac{[B]}{[A]}\right) + R_{mix}}{2 + R_{mix}\left(\frac{[B]}{[A]}\right)} \tag{10}$$

With an equation that links R_B and R_{mix} to measurable quantities, it is possible to proceed with experimental

https://doi.org/10.1021/jacsau.4c00628
JACS Au 2024, 4, 4273−4284

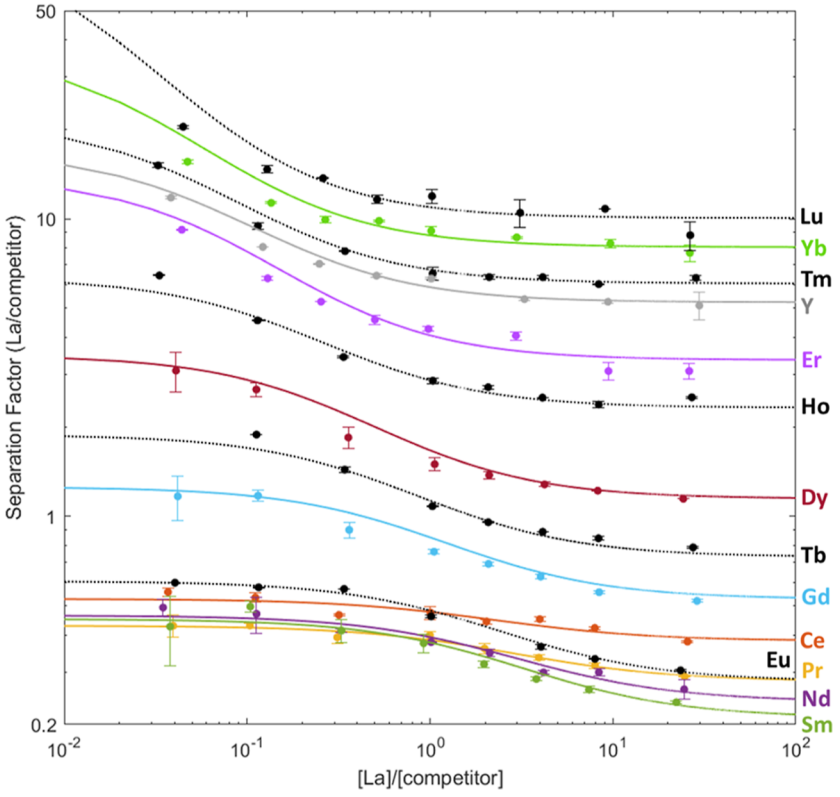

Figure 2. SF for all binary REE pairs containing La tested here. The SF was determined using agarose-immobilized LanM at REE ion ratios for La/competitor from approximately 1:24 to 27:1. Solid and dashed lines depict the model fit to the experimental data. Error bars show results in duplicate.

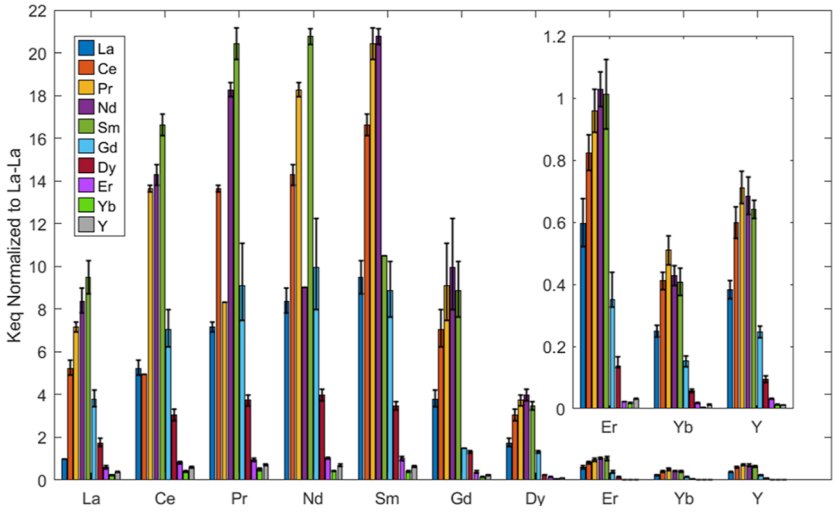

Figure 3. Equilibrium constants normalized to La−La for all possible combinations of the 10 studied REEs. Error bars are derived from a sensitivity analysis in which the heterogeneous constant was adjusted above and below the optimum value as necessary to double the sum of squared errors. Full details on the sensitivity analysis are shown in the Supporting Information (Figure S12). The homogeneous ion equilibrium constants agree well with the values measured for free LanM.[9]

validation. As this equation would suggest, it is possible to determine the relative binding constants, R_B and R_{mix}, by determining the SF of immobilized LanM at various binary ion ratios. As such, our experimental validation focuses on characterizing the SF of the 55 binary pairs comprising any pair of the eight REEs—La, Ce, Pr, Nd, Sm, Gd, Dy, Er, Yb, and Y—across a range of binary ion ratios. Additionally, all adjacent pairs (e.g., Gd−Tb and Tb−Dy) as well as a few pairs in the heavy REE range were characterized.

RESULTS

To facilitate the characterization of LanM complexation with heterogeneous ion pairs, we immobilized LanM onto agarose as previously described.[11] The use of immobilized LanM provides a facile means of separating REEs bound to LanM from the bulk REE solution, allowing SF determination. Agarose-LanM was partitioned into 96-well plates and equilibrium metal binding assays were conducted for 55

https://doi.org/10.1021/jacsau.4c00628
JACS Au 2024, 4, 4273−4284

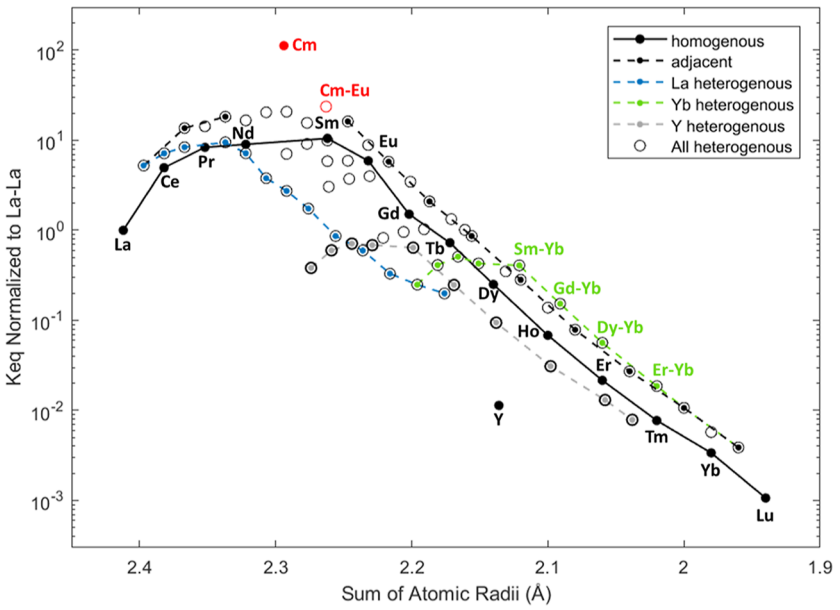

Figure 4. Effect of ionic radii on LanM-REE complex stability. Plot showing the relationship between the sum of ionic radii (coordination number 9)[22] and relative equilibrium constants normalized to the equilibrium constant for the La−La complex. Heterogeneous pairs of similar ions are generally tighter-binding than predicted by interpolation between homogeneous binding constants. Y-containing heterogeneous pairs bind more weakly than similar heterogeneous pairs containing two lanthanides. The equilibrium constants for the homogeneous curium (Cm)—Cm pair and the heterogeneous Cm−Eu pair are shown for reference.

binary pairs comprising any pair of 10 trivalent REEs—La, Ce, Pr, Nd, Sm, Gd, Dy, Er, Yb, and Y—in eight concentration ratios ranging from 1:24 to 27:1. Additionally, all adjacent pairs (e.g., Gd−Tb and Tb−Dy) as well as a few pairs in the heavy REE range (i.e., Tm−Lu) were characterized. SF for REE ion pairs were determined after quantifying the concentration of each REE bound to LanM using by inductively coupled plasma mass spectrometry (ICP−MS) following a desorption step. The experimental data and model fits for the representative REE La are shown in Figure 2, while the data for the other REEs are included in Figures S1−S10.

Although the SF plots for all binary pairs were unique, there were certain common characteristics. In all cases, the SF for each REE pair was dependent on the relative concentration ratio, with the SF the highest when the ratio of strong/weak binding ion was at its lowest. For example, the $SF_{La/Dy}$ was 3.0 when weaker binding ion Dy was in 30-fold excess of La, but only 1.1 when the tighter-binding ion La was 30-fold excess. As intuition would suggest, the SF was lower for ions that are adjacent on the periodic table (e.g., La−Ce) while SF was higher for more distant pairs (e.g., La−Yb). Samarium was the only ion that had a SF greater than unity with all competing ions, indicating that it is the most preferred ion for immobilized LanM, which is consistent with our prior data.[12] Interestingly, distant pairs of ions that bracket Sm presented with a generally low SF (e.g., La−Dy) or even displayed selectivity that inverted at a critical ion ratio (La−Gd, La−Tb). Importantly, these diverse and counterintuitive behaviors could all be captured by the model using the equilibrium constants shown in Table S1 to calculate the ratios of equilibrium constants R_B and R_{mix} for all pairs. The homogeneous binding constants shown on the diagonal in Table S1 were each used to fit several separate data sets, yielding an average error of less than 4% between model and experiment across all 64 ion pairs. This demonstrates that the model can coherently explain all the binary equilibration data. An example of the difference between a global and individual fit and an example of the sensitivity analysis are shown in Figures S11 and S12.

The model was then used to determine the equilibrium binding constants for all homogeneous and heterogeneous pairs (Figure 3). The trend in equilibrium constants for each ion pair generally agrees with data for LanM in free solution.[9] The Sm−Sm binding complex is the tightest binding homogeneous pair. Heavier (e.g., Yb−Yb) or lighter ion (e.g., La−La) pairs form less stable complexes. A key feature is that the three tightest binding homocomplexes are Sm, Nd, and Pr in descending order. Light elements La and Ce preferentially bind Sm, followed by Nd, followed by Pr. Heavy elements Er and Yb preferentially bind Pr, followed by Nd, followed by Sm. Gadolinium and Dy present an intermediate behavior in which they preferentially co-bind with Nd. This trend seems to indicate that there is an optimum co-binding of light and heavy ions that mimics the binding of tighter-binding homogeneous pairs.

Interestingly, many heterogeneous ion pairs form complexes more readily than homogeneous ion pairs—including Sm−Sm. This is likely because these binding constants are the sum of two equivalent binding complexes of the same ions in two different configurations. In other words, the possibility for two different ion configurations creates a statistical advantage for the formation of heterogeneous complexes. This intrinsic advantage for heterogeneous binding is unrelated to complex stability.

Sum of Ionic Radii Predicts Complex Stability

The structural origins of LanM's intra-lanthanide selectivity are not yet fully understood, but likely involve a combination of differences in the ionic radius (and relatedly, coordination number), and underlying electronic structure.[10] Accordingly, in Figure 4, we plotted the La-normalized K_{eq} for all homogeneous and a subset of heterogeneous REE pairs against the sum of ionic radii of the ions. The black line

https://doi.org/10.1021/jacsau.4c00628
JACS Au 2024, 4, 4273−4284

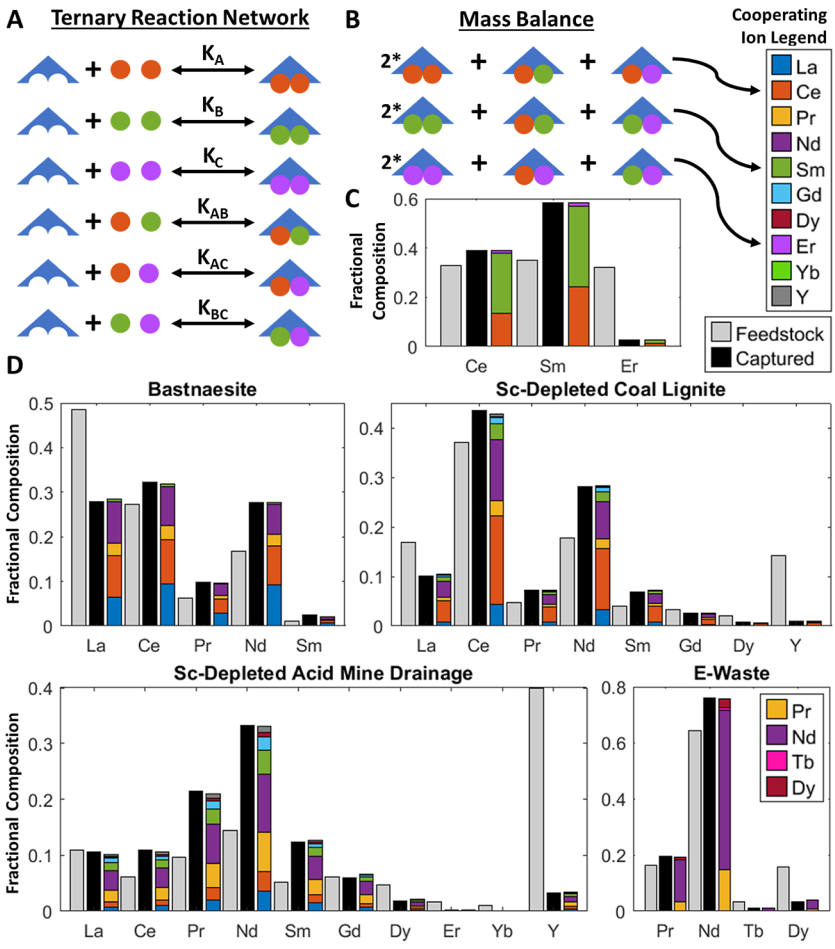

Figure 5. Plots showing the model fit for poly-ion equilibration experiments. (A) Reaction network showing how three ions compete for binding sites on LanM. (B) Mass balance showing how protein speciation, determined by solving a system of equations, is employed in a mass-balance to predict protein-bound composition. (C) Equimolar Ce−Sm−Er equilibration experimental results with model fits shown as a stacked bar showing how the protein speciation mass balance leads to the model prediction. Each segment of the stacked sum shows the fraction of the ion that is cooperatively bound with the ion of its corresponding color in the legend. (D) Poly-ion model predictions and experimental results for several common feedstocks (synthetic solutions). The gray bars depict the REE ion composition in the feedstock.

connects all homogeneous ion pairs, with heterogeneous points falling above this line having a higher K_{eq} for a corresponding sum of ionic radii, while those falling below the line have a lower K_{eq} for a corresponding sum of ionic radii. From this plot, it is readily apparent that there is an optimal sum of ionic radii, similar to the parabolic selectivity curve of LBTs.[8] Unlike LBTs, the selectivity strongly favors light lanthanides similar to recent work on bis-lactam and macrocyclic ligands.[20,21]

Overall, our results show that ionic radius is a good predictor of complexation strength and reveal important insights into the mixed binding preferences of LanM (Figure 4). First, complexes with adjacent ions, labeled by the dashed black line in Figure 4, appear to be nearly exactly 2-fold higher than the linear interpolation between homogeneous binding constants. This precise 2-fold increase serves as further evidence of the statistical benefit of hetero-ion complexation. Second, ion pairs with smaller size disparities appear closer to the linear interpolation between homogeneous binding constants than those with larger size disparities. For example, complexes of highly dissimilar sized ion pairs, as shown by the La-hetero and Yb-hetero (Yb−La through Yb−Nd) pairs marked by the blue and magenta dashed lines, respectively, fall below the homogeneous line. One possible explanation for this difference in behavior is that the ion complexes that have the largest disparity in ion sizes favor one orientation over another (i.e., P*AB vs P*BA). However, this explanation alone would only explain the reduction of heterogeneous complexation to be equivalent to that of a homogeneous ion complex. Alternatively, a portion or the entirety of these differences may result from variations in the relative stability of single-ion complexes. It may be possible to account for this effect by employing a partial cooperativity model in which the perfect cooperativity stability constants are the product of two sequential reactions to form the single-ion complex and two-ion complex in series with two distinct stability constants (i.e., a Klotz-type binding model). Due to the nature of our ICP−MS based experiments, it is not possible to deconvolve the relative binding strength of different binding configurations (i.e., P*AB vs P*BA). However, future work to characterize homogeneous and heterogeneous LanM complexes by crystallography, molecular dynamics modeling, or experimental determination of complexation kinetics may allow for the validation of a Klotz-type binding model that would address these questions.

Y-hetero pairs (and the Y−Y homogeneous pair) fall well below the homogeneous line. We attribute this to relative weakness of Y complexation relative to lanthanides. While

https://doi.org/10.1021/jacsau.4c00628
JACS Au 2024, 4, 4273−4284

many of yttrium's physical properties such as ionic radius and electronegativity are comparable to the lanthanides, Y notably does not have any 4f electrons. Weaker binding of Y^{3+} relative to lanthanides of similar ionic radius (Dy^{3+}, Ho^{3+}) has been observed in LanM, as well as in other chelators.[11,13] Recent research with small-molecule ligands suggests that such effects may arise from greater covalency in metal−ligand bonds involving lanthanide ions.[23,24] However, this topic requires further study.

Finally, Yb-Ln mixed complexes are stronger than would be predicted when compared to other lanthanides. For example, Yb−Sm, Yb−Gd, and Yb−Dy exhibit unexpectedly high K_{eq} values, falling above the linear interpolation between adjacent binding constants. This trend is observed to a lesser degree for Er, but not for Dy. We speculate that this may be because Yb^{3+} (and perhaps also Er^{3+}) binds with a lower CN, potentially removing a water molecule from the binding pocket or even decreasing the effective number of carboxylate groups coordinating to the Yb^{3+} ion. This would, in theory, increase the degrees of freedom for the other EF-hand to conform around the lanthanide ion and enhance mixed binding. Indeed, a recent quantum mechanics and molecular dynamics study predicts a decrease in the coordination number from 9 to 8 for LanM-bound lanthanides from Ho^{3+} to Lu^{3+}.[25] Further structural studies are needed to prove that LanM favors heterogeneous ion pairs with unequal coordination numbers.

Extending the Model to a Lanthanide-Actinide Complex

The cooperative binding of lanthanides and actinides to LanM provides a useful test case for this model. Previously reported separation data shows that the SF is enhanced at higher concentrations of the stronger-binding ion (the actinide, curium) relative to the weaker-binding ion (the lanthanide, europium).[26] Despite the differences between lanthanide and actinide chemistry, the perfect cooperativity model could be fit to these separation data with less than 5% error (Figure S13). The resulting curve shape, which is opposite to the typical lanthanide−lanthanide separation behavior, is the result of a highly disfavored mixed binding complex (R_B = 19 and R_{mix} = 4; Figure 4). LanM does not express such a wide disparity between R_B and R_{mix} until much higher R_B values in lanthanide−lanthanide separations. Interestingly, a variant of LanM containing an aspartate to asparagine substitution at position nine of EF hands 1−3 ($3D_9N$[26]) disfavors mixed binding between Cm and Eu to an even greater degree (R_B = 60 and R_{mix} = 5.8), consistent with its higher Cm vs Eu SF.

Applying the Model to Predict Poly-Ion Separations

Accounting for LanM's nonintuitive separation properties grows into an infinite task when trying to design capital projects for the widely varied REE composition in ore leachates and e-waste streams. As such, the goal of this model is to predict how immobilized LanM differentially binds REE ions from complex mixtures. The system of equations used to describe the binary separation was expanded to include up to ten ions as shown in the Supporting Information. The system of equations was then solved for various combinations of all eight REE ions and compared to experimental results for the same ion mixtures. Critically, despite being built from data generated with only binary REE pairs, the model was able to accurately predict the adsorption of ions in various equimolar solutions of three, four, and five REE ions (Figures S14−S16). Moreover, the bulk ion binding prediction was derived from a mass balance on the protein complex speciation which cannot be directly determined through experiment. This shows that the model is capable of providing insights that are inaccessible with experiment alone. Most importantly, as shown in Figure 5, the model was also able to accurately predict the adsorption of ions in various synthetic solutions mimicking the REE composition of real-world feedstocks, including acid mine drainage, bastnaesite, lignite coal, and E-waste leachates.[27−30] Where applicable, the test solutions modeled Sc-depleted feedstocks because there are existing methods to selectively remove Sc from solution.[31] These results demonstrate that the perfect cooperativity model is capable of predicting separation for a wide variety of ion mixtures. Beyond its application to industrial separations, the accuracy of poly-ion separation predictions demonstrates that the perfect cooperativity model is an accurate mechanistic description of how LanM complexes with lanthanides.

DISCUSSION

Being a protein, LanM stands in contrast to industrial REE chelators. It is much larger in size and consists of flexible and structured regions that work in tandem to form stable complexes with REE ions. It also possesses multiple REE binding sites. This structural complexity results in cooperative binding.[9,14] While LanM's cooperative binding characteristic is unprecedented in small-molecule chelators, many biomolecules possess cooperative binding characteristics, including its well-known homologue, calmodulin, for Ca(II), and the archetypal cooperative binding protein, hemoglobin, for O_2. Calmodulin (CaM), binds four calcium ions per molecule with two sets of two EF-hands that each bind Ca(II) ions in a highly cooperative manner.[32] While CaM is known to bind metal ions other than Ca(II), to the best of our knowledge, there is only one example in the literature for quantifying mixed binding of two ions, Mg(II) and Ca(II), simultaneously.[16] Indeed, Malmendal et al. based their calculations on a reduced-complexity version of the same full reaction network we present in Figure 1, although they allow for 2-step complexation of homo-ion complexes while resorting to a 1-step complexation simplification only for the hetero-ion complex.[16] Meanwhile, a structural study of the Na(I)−Ca(II) exchanger, another EF-hand protein, confirmed that mixed binding of Ca(II) and Mg(II) in a specific orientation was the thermodynamically preferred state for the protein.[33] LanM presents an additional layer of complexity because it strongly binds many different ions possessing similar physical properties. Unlike prior work characterizing the mixed binding of a single pair of ions to EF-hand proteins, our study quantified LanM's affinity for 64 heterogeneous ion pairs. As such, this study may provide clues to help elucidate competition dynamics in other cooperative binding proteins such as hemoglobin, and a variety of ligand-mediated ion channels such as the muscarinic acetylcholine receptor.[34]

The results of this analysis yield several nonintuitive results that are captured by the thermodynamic model. For all ion pairs, separation is hindered when the tighter-binding ion is more abundant than the weaker-binding ion based on the homogeneous binding constant (Figure 2). A particularly pronounced example of this effect is the Dy−La pair that has little to no separation at high La/Dy ratios, compared to a SF > 3 at high Dy/La ratios. The La−Tb pair demonstrates the more unusual behavior that LanM selectivity reverses to favor the ion that is less abundant in the mobile phase. This effect is driven by the relatively high heterogeneous La−Tb equilibrium

https://doi.org/10.1021/jacsau.4c00628
JACS Au 2024, 4, 4273−4284

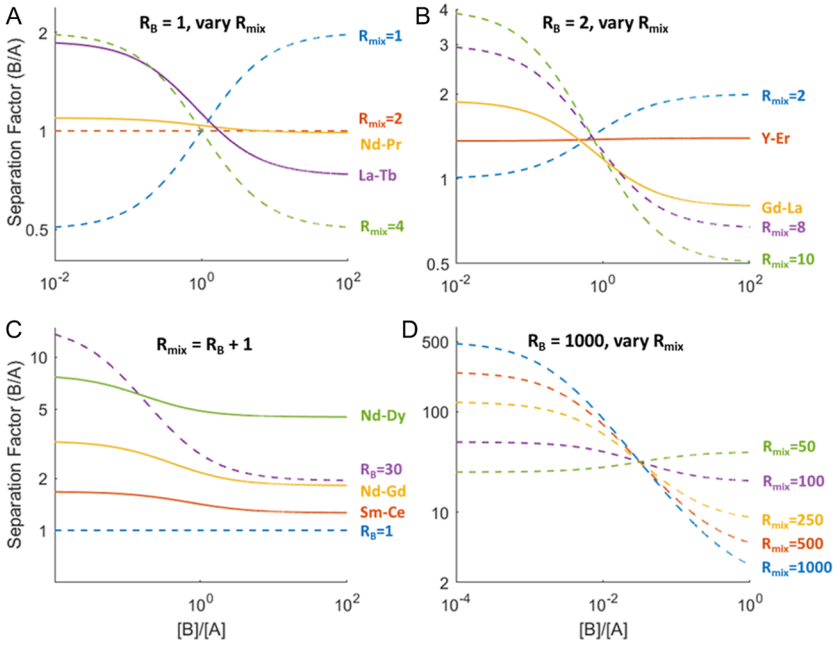

Figure 6. Hypothetical scenarios for LanM's separation performance. (A) Plot showing how mixed binding affects separation when homogeneous binding constants are equal. (B) Plot showing how mixed binding affects separation when homogeneous binding constants differ by a factor of 3. (C) Plot showing how separation varies when $R_{mix} = R_B + 1$. (D) Plot showing how mixed binding affects separation, especially at low B/A ratios, when mixed binding constants are separated by a factor of 1000.

constant which is over four times greater than either of the two homogeneous binding constants. Consequently, LanM serves to actively mix La with heavy REEs like Gd, Tb, and Dy rather than separate them. To overcome LanM's propensity to mix light and heavy REEs, complementary separation modalities are necessary. While such a complementary separation technique may take the form of a separate unit operation, such as a mixer-settler step or a column with different REE selectivity, it is also possible to employ chelators in a "ligand tug-of-war strategy" similar to what has been recently demonstrated.[35] Dong et al. demonstrated what may be described as a protein−ligand tug-of-war when the selectivity of citrate for heavy REEs was used synergistically with immobilized LanM to enhance the separation of Nd and Dy.[11] More recently, this approach was extended for La and Dy separation.[15]

To conceptionally demonstrate how mixed binding affects binary metal ion separations, we used our model to explore several hypothetical scenarios with different binding constants for homogeneous and heterogeneous pairs of competing ions (Figure 6). Scenario A shows how mixed binding affects separation when the two homogeneous binding constants are identical, a scenario similar to La and Tb (Figure 6A). When the mixed binding constant (R_{mix}) is twice the homogeneous binding constants, there is no separation. This is a reasonable result because it shows that if there is no preference between any of four possible protein complexes, there will be no separation. When the mixed binding constant is either increased or decreased relative to the homogeneous binding constants (i.e., $R_{mix} > 2$ or $R_{mix} < 2$), separation becomes possible, but reverses preference on either side of a 1:1 ion ratio.

Scenario B shows how mixed binding alters separation when two ions have moderately different homogeneous equilibrium constants ($R_B = K_B/K_A = 2$) (Figure 6B). This is intended to explore the role of mixed binding in generating the counterintuitive SF inversion effect that occurs for some ion pairs that are on opposite sides of Sm in the lanthanide series (i.e., light vs heavy REEs). These hypothetical scenarios align with and extrapolate beyond the real examples of ion pairs with greater heterogeneous binding constants than either of the respective homogeneous binding constants (Gd−La, Ce−Gd, etc.). Moreover, these ion pairs show a pattern of moving closer by a single ion (e.g., La−Dy → Ce−Gd) on either side of a center point between Nd and Sm. This result suggests that Nd and Sm are bracketing the true optimally binding ion, Pm. Furthermore, we hypothesize that the tightest binding ion pair would be the combination of Pm and Sm. Indeed, recent work characterizing the complexes of Pm with a diglycolamide ligand confirms that Pm complexation geometry and energetics fits predictably into the wider lanthanide series, providing additional support for this theory.[36]

Scenario C shows what happens when the difference in homogeneous binding constants for two ions is progressively increased while the mixed binding constant is defined as the sum of the two homogeneous binding constants (Figure 6C). When this condition, $K_{mix} = K_A + K_B$, is normalized by dividing both sides by K_A, it can be found that $R_{mix} = R_B + 1$. This is a common scenario in our results when two ions are in proximity to one another in the lanthanide series and are not on opposing sides of Sm. This scenario shows that the SF hits a ceiling at 3 when the tighter-binding ion is in excess of the weaker-binding ion regardless of how great the difference is between homogeneous SF. While there is a benefit to separation at low ratios of strong/weak binding ions, this shows that mixed binding, as it currently manifests for LanM, imposes a strong separation performance limitation for both adjacent and closely spaced REE ions. This separation dampening effect can be observed even for moderately distant pairs such as Nd/Gd (R_B = 5.3 and R_{mix} = 5.6), where the SF is 2 at an equimolar concentration of ions despite the 5-fold difference in homogeneous binding constants. As such, a

https://doi.org/10.1021/jacsau.4c00628
JACS Au 2024, 4, 4273−4284

comparison of homogeneous binding constants alone will overestimate the separation potential for a particular REE pair.

In contrast to the scenario for closely spaced ions, mixed binding is disfavored in the most distantly spaced ions, with a prime example being the Nd−Dy pair with R_B = 31.7 and R_{mix} = 12.5. As expected, the Nd−Dy pair breaks the SF ceiling of 3, and instead plateaus just over 5 for high Nd−Dy ratios (Figure 6C). This suggests that when the difference in homogeneous binding constants is increased beyond a certain threshold, mixed binding becomes less pronounced (i.e, is no longer proportional). As such, there exists the possibility for nonlinear gains in separation performance if sufficiently large R_B can be achieved or if mixed binding can be further disfavored at a fixed R_B. This latter scenario could perhaps be achieved by strengthening the intraprotein interactions at the EF hand 2/3 interface to increase the rigidity of the EF hand domains. Indeed, highly rigid chelators built around a bis-lactam phenanthroline core have been employed to better discriminate between similarly sized REEs.[20,37] Ultimately, it remains to be seen whether engineering of LanM would allow for separation of closely related ions with performance similar to the Nd−Dy pair.

Scenario D explores the effect of mixed binding when one ion is favored over another by a factor of 1000, particularly when the weaker-binding ion is highly in excess of the stronger-binding ion (Figure 6D). This is intended to explore how LanM or a less REE-selective ancestor performs its natural cellular role, as lanthanides are up to 10000-fold less abundant in the environment compared to other abundant competitors (e.g., Ca).[38] While intuition would suggest that mixed binding, for example La−Ca, is detrimental to lanthanide recovery, this result shows that the opposite may be true. At very high excess of the nonlanthanide, strong mixed binding is predicted to improve the performance of LanM or its ancestral homologues, which might have had a physiological benefit in the host microbe's natural environment. Furthermore, the perfect cooperativity model implies LanM may have never faced evolutionary pressure to disfavor mixed binding between lanthanides as methylobacteria can utilize multiple lanthanide ions.

Regardless of the source of selective pressure, it appears likely that selectivity against Ca and heavy lanthanides are coupled. This is likely because Ca binds to ligands with a coordination number of 6 to 8, with recent computational work showing that Ca binds to CaM EF-hands with a coordination number of 7.[39] Similarly, heavy lanthanides are expected to bind to LanM with a lower coordination number than light lanthanides due to steric restraints around the smaller ion. Indeed, we show that a LanM variant (proline to alanine at position two of each EF hand; $4P_2A$) with 100-fold lower Ln/Ca selectivity exhibits a marked shift in selectivity toward heavier REEs with a pronounced reduction in selectivity for La, consistent with but extending prior data (Figure S17).[9]

When considering the physiological implications of the selectivity trends determined herein, it is important to caveat that our data do not include contributions from EF-hand 1, the weaker EF-hand domain that is active in free LanM but not in the immobilized protein. The contributions of this domain could be determined in subsequent work by expanding the modeling approach to include equations that predict the behavior of EF-hand 1 and collecting SF data for the free protein using spin filter assays.[26] Nevertheless, we have accurately characterized the selectivity of the highest-affinity EF-hands, which we expect to be generally transferable to the free protein.

We are left searching for an explanation for why LanM preferentially binds Sm (or perhaps more accurately, Pm), an element that is less abundant in nature compared to La, Ce, and Nd and does not have a clear biological function (at least in methanol oxidation) in *M. extorquens*. Indeed, there is evidence showing that the kinetic efficiency of XoxF-type methanol dehydrogenase enzymes decreases markedly from La through Nd,[40−42] with a clear reduction in growth efficiency on lanthanides evident for Nd and beyond.[43] Thus, the selectivity of LanM within the LREEs (La < Ce < Pr < Nd < Sm) is the inverse of the usability by XoxF. We thus speculate that LanM may play a role in sequestering Nd/Sm[44], which co-occur in the environment with the catalytically preferred lanthanides La and Ce, from XoxF. Indeed, a cellular mechanism for selective metalation of XoxF with La over Nd is supported by work by Nakagawa and co-workers showing that XoxF isolated from *M. extorquens* cells grown on equimolar amounts of Nd and La achieves a La/Nd loading ratio of 9:1.[45] Confirmation of this role requires additional work, including the elucidation of its cellular interacting partners. It will also be interesting to determine whether the selectivity of orthologous LanM and XoxF pairs exhibit an inverted selectivity trend. For example, the recently characterized LanM from *Hansschlegelia quercus* (*H. quercus*) achieves a selectivity profile shifted even further to the light REEs (peak at Pr[10]), raising the possibility that the corresponding XoxF may be more finely tuned for the lightest REEs, perhaps reflecting a different ecological niche.

CONCLUSION

The perfect cooperativity model of immobilized *M. extorquens* LanM has allowed for the determination of binding coefficients for heterogeneous ion pairs based on binary ion adsorption experiments. These constants then allowed for the accurate prediction of selective adsorption of REE ions from more complex mixtures. While the trend in binding constants initially showed that most ion pairs follow a simple trend of optimum binding for a certain sum of ionic radii, heterogeneous ion pairs with large differences in ionic radii formed less stable complexes than pairs closer in size. Future work to characterize hetero-ion complexes by molecular dynamics simulations and crystallography may help resolve more details about the structure−function relationship of LanM and enable rational engineering of more selective variants. Similarly, complementary analytical methods may enable the validation of a more mechanistically thorough model including separate equilibrium constants for single-ion complexation and single-to-double ion complexation. It will also be important to extend the thermodynamic characterization to natural orthologs and synthetic variants beyond the archetypal LanM, such as *H. quercus* LanM, which exhibits lanthanide-dependent dimerization and a substantially enhanced selectivity between LREEs and HREEs, the thermodynamic basis for which remains incompletely understood.

METHODS

Agarose LanM Immobilization

Purification and immobilization of *M. extorquens* LanM was performed using a thiol-maleimide conjugation reaction as previously reported.[11]

https://doi.org/10.1021/jacsau.4c00628
JACS Au 2024, 4, 4273−4284

96-Well Filter Plate Binary Equilibration Assay

Approximately 30 μL of agarose-LanM was distributed into each well of a 96-well filter plate. The agarose-LanM was first equilibrated with 10 mM MES buffer at pH 6 and then each well was repeatedly incubated with binary mixtures of REEs at concentration ratios ranging from 1:24 to 27:1 with a total concentration of 10 mM. After incubation the immobilized protein was thoroughly washed with water to remove any unbound ions. Finally, the LanM-bound REEs were desorbed by addition of 100 mM HCl. The desorbed REE composition was then analyzed by ICP−MS.

The aqueous compositions tested included binary pairs from all 45 possible binary combinations of ten representative REEs tested (as well as binary pairs selected from outside this set of ten ions) in eight ratios ranging from 1:24 to 27:1. Data analysis was performed using MATLAB to plot the SF function against experimental data. The function was fitted to data by modifying the constants R_B and R_{mix}. Fits for all binary pairs including La are shown in Figure 2. Plots for all binary pair fits are included in the Supporting Information. To ensure that the model was not overfitted to the data, relative equilibrium constants for homogeneous ion pairs were used as shared fitting parameters across all experiments.

ICP−MS Methods

Metal concentrations were determined ICP−MS using an Agilent ICP−MS 7850 system in helium mode. ICP−MS samples of the metals were prepared by dilution to a final 2% HNO_3 solution prepared from deionized Milli-Q water and ultrapure HNO_3 Optima (Fisher Chemical: S020101TFIF01). Metal calibration curves were created using gravimetrically prepared REE standards (Sigma-Aldrich: 67349) at 0, 0.0305, 0.122, 0.488, 1.953, 7.812, 31.25, 125, and 500 ppb (seven 1:4 dilutions of 500 ppb, with a 0 ppb blank prepared using the same matrix). Rhenium was used as an internal standard (Inorganic Ventures: CGRE1), a 1 ppb Tuning Solution was used for tuning (Agilent: 5185−5959), and 0.2 μm filtered Milli-Q water was used for probe washing. All sample measurements were corrected automatically for variation in the internal standard signal in the ICP−MS MassHunter software.

Thermodynamic Model Fitting

ICP−MS data was first processed in excel to convert ppm concentrations to molarity and determine the SF at each aqueous ion ratio. The processed data was then imported in MATLAB and fitting constants R_B and R_{mix} were optimized to minimize the sum of squared error relative to the average of duplicate results using the fminsearch function. All adjacent pairs (La−Ce, Ce−Nd, Nd−Sm, etc.) of ions were analyzed first because their lower SF were expected to be more precisely determined. The R_B values from these fits were then used to determine the K_{eq} for all homogeneous ion pairs relative to the La−La complex. These K_{eq} values were then used to calculate R_B values for all other ion pairs, and the R_{mix} value was optimized to minimize error. R_{mix} values for all pairs were then used to determine K_{eq} values normalized against the La−La complex. The resulting K_{eq} values for all homogeneous and heterogeneous ion pairs were then aggregated in the matrix shown in Table S1.

Poly-Ion Experiments and Modeling

Many equimolar 3-, 4-, and 5-ion solutions were prepared at pH 5.0 to include many possible combinations of ions (Figures S14−S16). These solutions were then incubated with LanM agarose in the same manner as the binary solutions. Both the HCl LanM desorbate and the residual solutions were analyzed by ICP−MS. The residual solution concentrations and the desorbate concentrations were imported into MATLAB as individual arrays for each result. The matrix of relative K_{eq} values was imported into MATLAB as a matrix. MATLAB functions were written to introduce K_{eq} values into systems of equations describing 3-, 4-, and 5-ion solutions binding to LanM. The system of equations was then solved using fsolve, resulting in the predicted composition of the LanM-metal complexes. The total protein-adsorbed fraction of each metal was determined by mass balance from the calculated LanM metal complexes. The results were then plotted alongside experimental results without any additional modification or fitting steps.

ASSOCIATED CONTENT

Supporting Information

The Supporting Information is available free of charge at https://pubs.acs.org/doi/10.1021/jacsau.4c00628.

Heterogeneous Binding (PDF)

AUTHOR INFORMATION

Corresponding Author

Dan M. Park − *Critical Materials Innovation Hub, Physical and Life Sciences Directorate, Lawrence Livermore National Laboratory, Livermore, California 94550, United States;* orcid.org/0000-0002-6000-6805; Email: park36@llnl.gov

Authors

Jeremy Seidel − *Critical Materials Innovation Hub, Physical and Life Sciences Directorate, Lawrence Livermore National Laboratory, Livermore, California 94550, United States*

Patrick Diep − *Critical Materials Innovation Hub, Physical and Life Sciences Directorate, Lawrence Livermore National Laboratory, Livermore, California 94550, United States;* orcid.org/0000-0001-9403-3206

Ziye Dong − *Critical Materials Innovation Hub, Physical and Life Sciences Directorate, Lawrence Livermore National Laboratory, Livermore, California 94550, United States;* orcid.org/0000-0002-0419-8523

Joseph A. Cotruvo, Jr. − *Department of Chemistry, The Pennsylvania State University, University Park, Pennsylvania 16802, United States;* orcid.org/0000-0003-4243-8257

Complete contact information is available at: https://pubs.acs.org/10.1021/jacsau.4c00628

Author Contributions

CRediT: **Jeremy Seidel** conceptualization, data curation, formal analysis, investigation, methodology, visualization, writing - original draft; **Patrick Diep** investigation, resources, writing - review & editing; **Ziye Dong** investigation, resources; **Joseph A. Cotruvo** funding acquisition, writing - review & editing; **Dan M. Park** conceptualization, funding acquisition, project administration, supervision, writing - original draft.

Notes

The authors declare the following competing financial interest(s): Z.D., J.A.C., and D.M.P. are listed as inventors on a related patent application submitted by Lawrence Livermore National Laboratory and the Pennsylvania State University.

ACKNOWLEDGMENTS

This research is supported by the Critical Materials Innovation Hub, an Energy Innovation Hub funded by the U.S. Department of Energy, Office of Energy Efficiency and Renewable Energy, Advanced Materials & Manufacturing Technologies Office. J.A.C. also acknowledges support from the U.S. DOE (DE-SC0021007 to J.A.C.). This work was performed under the auspices of the U.S. Department of Energy by Lawrence Livermore National Laboratory under Contract DEAC52-07NA27344 (LLNL-JRNL-867791).

REFERENCES

(1) technavio. *Rare Earth Metals Market by Application, Type, and Geography- Forecast and Analysis 2023−2027*, December 2022.
(2) Gupta, C. K.; Krishnamurthy, N. Extractive metallurgy of rare earths. *Int. Mater. Rev.* **1992**, *37* (1), 197−248.
(3) Hidayah, N. N.; Abidin, S. Z. The evolution of mineral processing in extraction of rare earth elements using solid-liquid extraction over liquid-liquid extraction: A review. *Miner. Eng.* **2017**, *112*, 103−113.
(4) Franz, K. J.; Nitz, M.; Imperiali, B. Lanthanide-binding tags as versatile protein coexpression probes. *Chembiochem* **2003**, *4* (4), 265−271.
(5) Park, D. M.; Reed, D. W.; Yung, M. C.; Eslamimanesh, A.; Lencka, M. M.; Anderko, A.; Fujita, Y.; Riman, R. E.; Navrotsky, A.; Jiao, Y. Bioadsorption of Rare Earth Elements through Cell Surface Display of Lanthanide Binding Tags. *Environ. Sci. Technol.* **2016**, *50* (5), 2735−2742.
(6) Park, D. M.; Brewer, A.; Reed, D. W.; Lammers, L. N.; Jiao, Y. Recovery of Rare Earth Elements from Low-Grade Feedstock Leachates Using Engineered Bacteria. *Environ. Sci. Technol.* **2017**, *51* (22), 13471−13480.
(7) Chang, E.; Brewer, A. W.; Park, D. M.; Jiao, Y.; Lammers, L. N. Surface complexation model of rare earth element adsorption onto bacterial surfaces with lanthanide binding tags. *Appl. Geochem.* **2020**, *112*, 104478.
(8) Nitz, M.; Sherawat, M.; Franz, K. J.; Peisach, E.; Allen, K. N.; Imperiali, B. Structural origin of the high affinity of a chemically evolved lanthanide-binding peptide. *Angew. Chem., Int. Ed.* **2004**, *43* (28), 3682−3685.
(9) Cotruvo, J. A., Jr.; Featherston, E. R.; Mattocks, J. A.; Ho, J. V.; Laremore, T. N. Lanmodulin: A Highly Selective Lanthanide-Binding Protein from a Lanthanide-Utilizing Bacterium. *J. Am. Chem. Soc.* **2018**, *140* (44), 15056−15061.
(10) Mattocks, J. A.; Jung, J. J.; Lin, C.-Y.; Dong, Z.; Yennawar, N. H.; Featherston, E. R.; Kang-Yun, C. S.; Hamilton, T. A.; Park, D. M.; Boal, A. K.; Cotruvo, J. A., Jr. Enhanced rare-earth separation with a metal-sensitive lanmodulin dimer. *Nature* **2023**, *618* (7963), 87−93.
(11) Dong, Z.; Mattocks, J. A.; Deblonde, G. J.-P.; Hu, D.; Jiao, Y.; Cotruvo, J. A., Jr.; Park, D. M. Bridging Hydrometallurgy and Biochemistry: A Protein-Based Process for Recovery and Separation of Rare Earth Elements. *ACS Cent. Sci.* **2021**, *7* (11), 1798−1808.
(12) Dong, Z.; Mattocks, J. A.; Seidel, J. A.; Cotruvo, J. A., Jr.; Park, D. M. Protein-Based approach for high-purity Sc, Y, and grouped lanthanide separation. *Sep. Purif. Technol.* **2024**, *333*, 125919.
(13) Deblonde, G. J.-P.; Mattocks, J. A.; Park, D. M.; Reed, D. W.; Cotruvo, J. A., Jr.; Jiao, Y. Selective and Efficient Biomacromolecular Extraction of Rare-Earth Elements using Lanmodulin. *Inorg. Chem.* **2020**, *59* (17), 11855−11867.
(14) Featherston, E. R.; Issertell, E. J.; Cotruvo, J. A., Jr. Probing Lanmodulin's Lanthanide Recognition via Sensitized Luminescence Yields a Platform for Quantification of Terbium in Acid Mine Drainage. *J. Am. Chem. Soc.* **2021**, *143* (35), 14287−14299.
(15) Hussain, Z.; Kim, S.; Cho, J.; Sim, G.; Park, Y.; Kwon, I. Repeated Recovery of Rare Earth Elements Using a Highly Selective and Thermo-Responsive Genetically Encoded Polypeptide. *Adv. Funct. Mater.* **2022**, *32* (13), 2109158.
(16) Malmendal, A.; Linse, S.; Evenäs, J.; Forsén, S.; Drakenberg, T. Battle for the EF-Hands: Magnesium−Calcium Interference in Calmodulin. *Biochemistry* **1999**, *38* (36), 11844−11850.
(17) Hill, A. V. The possible effects of the aggregation of the molecules of haemoglobin on its dissociation curves. *J. Physiol.* **1910**, *40*, 4−7.
(18) Adair, G. S.; Bock, A. V.; Field, H. The hemoglobin system: vi. The oxygen dissociation curve of hemoglobin. *J. Biol. Chem.* **1925**, *63* (2), 529−545.
(19) Klotz, I. M. The application of the law of mass action to binding by proteins; interactions with calcium. *Arch. Biochem. Biophys.* **1946**, *9*, 109.
(20) Healy, M. R.; Ivanov, A. S.; Karslyan, Y.; Bryantsev, V. S.; Moyer, B. A.; Jansone-Popova, S. Efficient Separation of Light Lanthanides(III) by Using Bis-Lactam Phenanthroline Ligands. *Chem.—Eur. J.* **2019**, *25* (25), 6326−6331.
(21) Thiele, N. A.; Fiszbein, D. J.; Woods, J. J.; Wilson, J. J. Tuning the Separation of Light Lanthanides Using a Reverse-Size Selective Aqueous Complexant. *Inorg. Chem.* **2020**, *59* (22), 16522−16530.
(22) Lundberg, D.; Persson, I. The size of actinoid(III) ions − structural analysis vs. common misinterpretations. *Coord. Chem. Rev.* **2016**, *318*, 131−134.
(23) Zhang, X.; Zhang, X.; Zheng, H.; Kuang, S.; Liu, X.; Liao, W. Yttrium separation by phosphorylcarboxylic acid and the underlying tetrad effect along lanthanide unveiled from different microscopic interactions. *Fundam. Res.* **2023**.
(24) Zanella, B. S.; Jones, S. B.; Lee, H.-S.; Hancock, R. D. Evidence for Participation of 4f and 5d Orbitals in Lanthanide Metal−Ligand Bonding and That Y(III) Has Less of This Complex-Stabilizing Ability. A Thermodynamic, Spectroscopic, and DFT Study of Their Complexation by the Nitrogen Donor Ligand TPEN. *Inorg. Chem.* **2022**, *61* (11), 4627−4638.
(25) Prejanò, M.; Toscano, M.; Marino, T. Periodicity of the Affinity of Lanmodulin for Trivalent Lanthanides and Actinides: Structural and Electronic Insights from Quantum Chemical Calculations. *Inorg. Chem.* **2023**, *62* (19), 7461−7470.
(26) Mattocks, J. A.; Cotruvo, J. A., Jr.; Deblonde, G. J.-P. Engineering lanmodulin's selectivity for actinides over lanthanides by controlling solvent coordination and second-sphere interactions. *Chem. Sci.* **2022**, *13* (20), 6054−6066.
(27) Zhang, W.; Honaker, R. Process development for the recovery of rare earth elements and critical metals from an acid mine leachate. *Miner. Eng.* **2020**, *153*, 106382.
(28) *Technical Report on the Arizona La Paz Rare Earths and Scandium Project*. 2020.
(29) Laudal, D. A.; Benson, S. A.; Addleman, R. S.; Palo, D. Leaching behavior of rare earth elements in Fort Union lignite coals of North America. *Int. J. Coal Geol.* **2018**, *191*, 112−124.
(30) Du, X.; Graedel, T. E. Global Rare Earth In-Use Stocks in NdFeB Permanent Magnets. *J. Ind. Ecol.* **2011**, *15* (6), 836−843.
(31) Brewer, A.; Reicher, C.; Manatschal, O.; Bai, H.; Nakanishi, K.; Kleitz, F. Powdered Hierarchically Porous Silica Monoliths for the Selective Extraction of Scandium. *ACS Sustainable Chem. Eng.* **2023**, *11* (42), 15432−15439.
(32) Iida, S.; Potter, J. D. Calcium Binding to Calmodulin. Cooperativity of the Calcium-Binding Sites. *J. Biochem.* **1986**, *99* (6), 1765−1772.
(33) Breukels, V.; Konijnenberg, A.; Nabuurs, S. M.; Touw, W. G.; Vuister, G. W. The Second Ca2+-Binding Domain of NCX1 Binds Mg2+ with High Affinity. *Biochemistry* **2011**, *50* (41), 8804−8812.
(34) Jakubík, J.; Bačáková, L.; El-Fakahany, E. E.; Tuček, S. Positive Cooperativity of Acetylcholine and Other Agonists with Allosteric Ligands on Muscarinic Acetylcholine Receptors. *Mol. Pharmacol.* **1997**, *52* (1), 172−179.
(35) Johnson, K. R.; Driscoll, D. M.; Damron, J. T.; Ivanov, A. S.; Jansone-Popova, S. Size Selective Ligand Tug of War Strategy to Separate Rare Earth Elements. *JACS Au* **2023**, *3* (2), 584−591.
(36) Driscoll, D. M.; White, F. D.; Pramanik, S.; Einkauf, J. D.; Ravel, B.; Bykov, D.; Roy, S.; Mayes, R. T.; Delmau, L. H.; Cary, S. K.; Dyke, T.; Miller, A.; Silveira, M.; VanCleve, S. M.; Davern, S. M.; Jansone-Popova, S.; Popovs, I.; Ivanov, A. S. Observation of a promethium complex in solution. *Nature* **2024**, *629* (8013), 819−823.
(37) Jansone-Popova, S.; Ivanov, A. S.; Bryantsev, V. S.; Sloop, F. V., Jr.; Custelcean, R.; Popovs, I.; Dekarske, M. M.; Moyer, B. A. Bis-lactam-1,10-phenanthroline (BLPhen), a New Type of Preorganized Mixed N,O-Donor Ligand That Separates Am(III) over Eu(III) with Exceptionally High Efficiency. *Inorg. Chem.* **2017**, *56* (10), 5911−5917.
(38) Voncken, J. H. L. *The Rare Earth Elements: An Introduction*; Springer, 2016.

https://doi.org/10.1021/jacsau.4c00628
JACS Au 2024, 4, 4273−4284

(39) Tan, Q.; Ding, Y.; Qiu, Z.; Huang, J. Binding Energy and Free Energy of Calcium Ion to Calmodulin EF-Hands with the Drude Polarizable Force Field. *ACS Phys. Chem. Au* **2022**, *2* (2), 143−155.
(40) Huang, J.; Yu, Z.; Chistoserdova, L. Lanthanide-Dependent Methanol Dehydrogenases of XoxF4 and XoxF5 Clades Are Differentially Distributed Among Methylotrophic Bacteria and They Reveal Different Biochemical Properties. *Front. Microbiol.* **2018**, *9*, 1366.
(41) Featherston, E. R.; Rose, H. R.; McBride, M. J.; Taylor, E. M.; Boal, A. K.; Cotruvo, J. A., Jr. Biochemical and Structural Characterization of XoxG and XoxJ and Their Roles in Lanthanide-Dependent Methanol Dehydrogenase Activity. *ChemBioChem* **2019**, *20* (18), 2360−2372.
(42) Phi, M. T.; Singer, H.; Zäh, F.; Haisch, C.; Schneider, S.; Op den Camp, H. J. M.; Daumann, L. J. Assessing Lanthanide-Dependent Methanol Dehydrogenase Activity: The Assay Matters. *ChemBioChem* **2024**, *25* (5), No. e202300811.
(43) Vu, H. N.; Subuyuj, G. A.; Vijayakumar, S.; Good, N. M.; Martinez-Gomez, N. C.; Skovran, E. Lanthanide-Dependent Regulation of Methanol Oxidation Systems in Methylobacterium extorquens AM1 and Their Contribution to Methanol Growth. *J. Bacteriol.* **2016**, *198* (8), 1250−1259.
(44) Larrinaga, W. B.; Jonathan, J. J; Lin, C.-Y.; Boal, A. K.; Cotruvo, J. A., Jr. *Modulating Metal-Centered Dimerization of a Lanthanide Chaperone Protein for Separation of Light Lanthanides*, 2024. Manuscript in revision.
(45) Wang, L.; Hibino, A.; Suganuma, S.; Ebihara, A.; Iwamoto, S.; Mitsui, R.; Tani, A.; Shimada, M.; Hayakawa, T.; Nakagawa, T. Preference for particular lanthanide species and thermal stability of XoxFs in Methylorubrum extorquens strain AM1. *Enzyme Microb. Technol.* **2020**, *136*, 109518.

https://doi.org/10.1021/jacsau.4c00628
JACS Au 2024, 4, 4273−4284